



The cyclic phase transformation concept and the effective interface mobility

E. Gamsjäger¹, Hao Chen², Sybrand van der Zwaag²

¹Montanuniversität Leoben, Institute of Mechanics, Leoben, Austria.

²Faculty of Aerospace Engineering, Delft University of Technology,
The Netherlands.



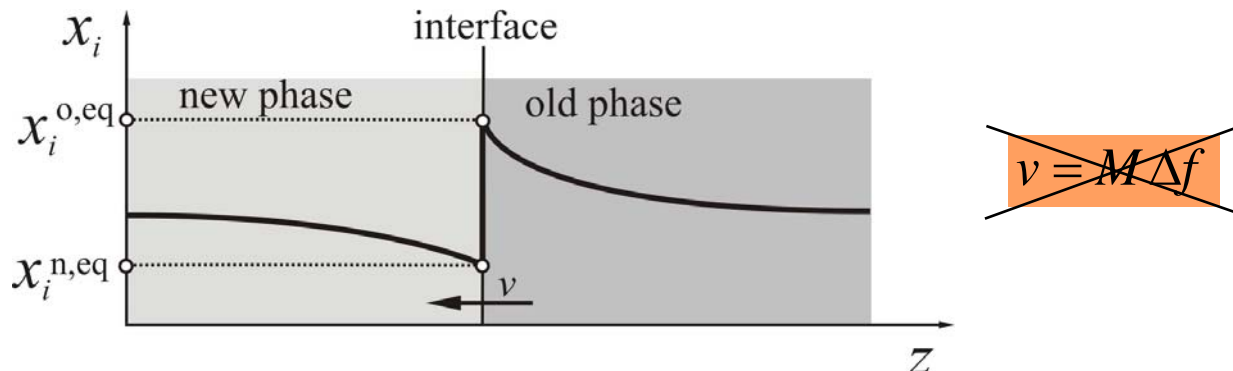
Contents

- **Motivation**
 - Diffusive phase transformations
(e.g. solid / liquid or solid/solid phase transformations)
- **Model 1 (LE)**
 - Modeling and experimental observations
- **Model 2 (thick interface) / Model 3 (effective interface mobility)**
 - Theory and modeling results
- **Model 1 / Model 3**
 - Cyclic phase transformations
- **Conclusions and Outlook**



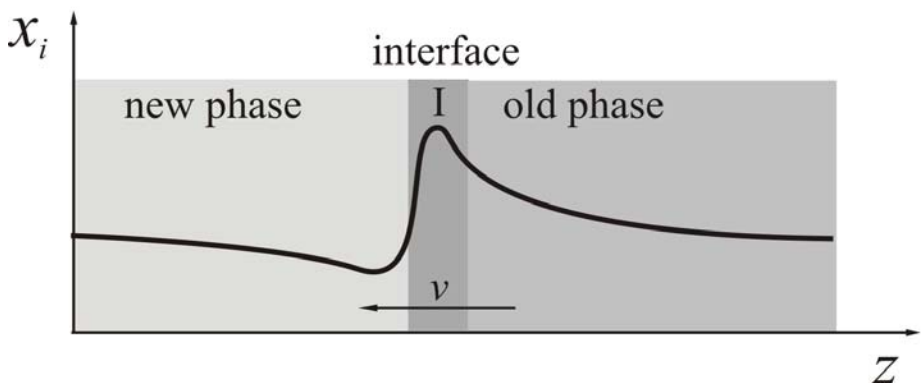
Theory

Model 1: Sharp interface, infinite mobility LE(NP)



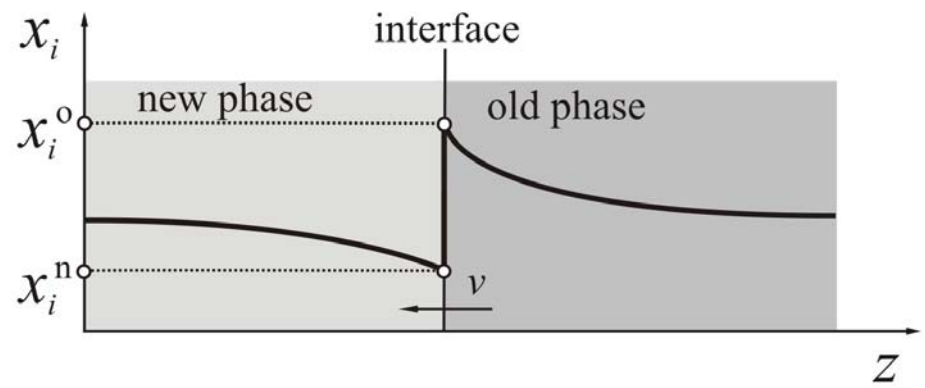
Model 2: Interfacial region

(Thick interface)



Model 3: Finite mobility (SI):

(Effective interface mobility, no substitutional bulk diffusion)

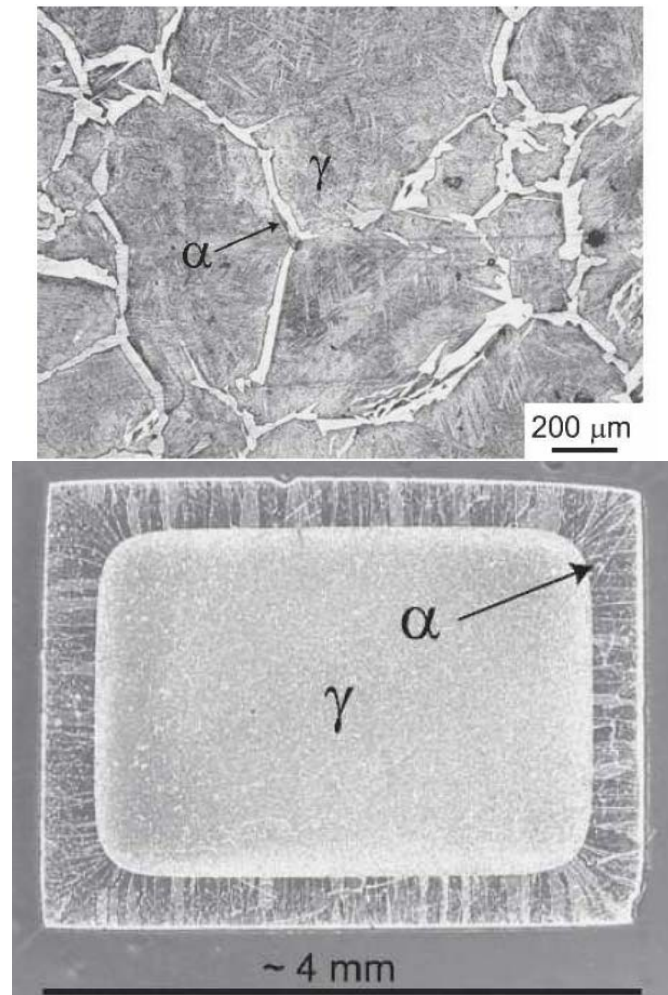
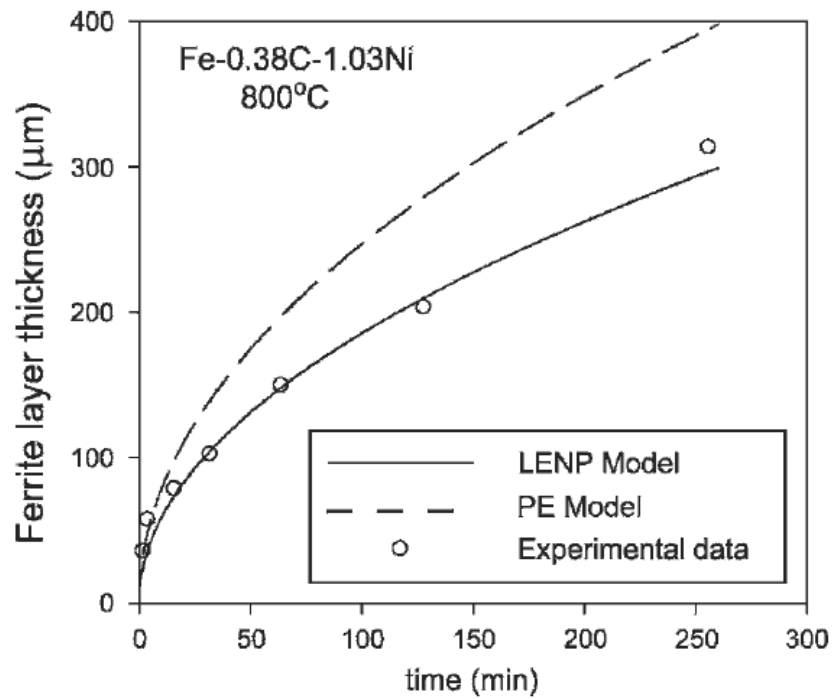


$$v = M \Delta f$$



Model 1: Sharp interface, infinite mobility LE(NP)

$\gamma \rightarrow \alpha$ transformation: Fe-C-Ni

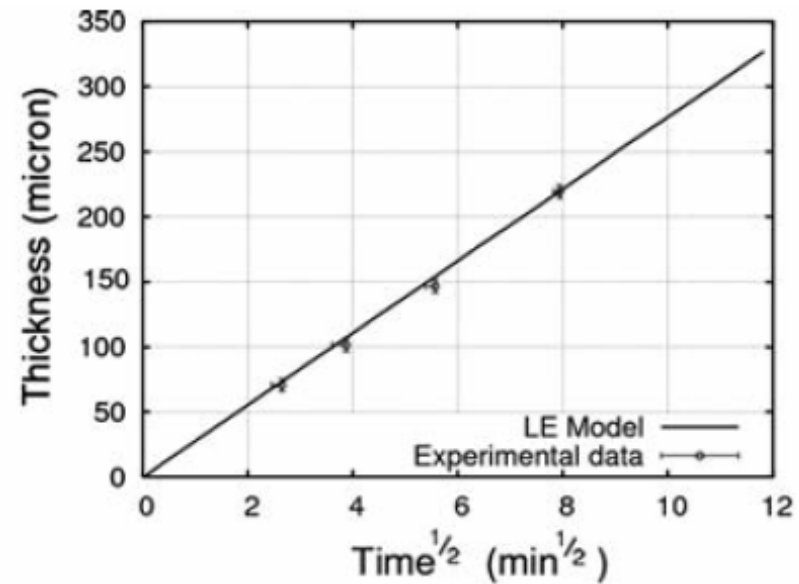
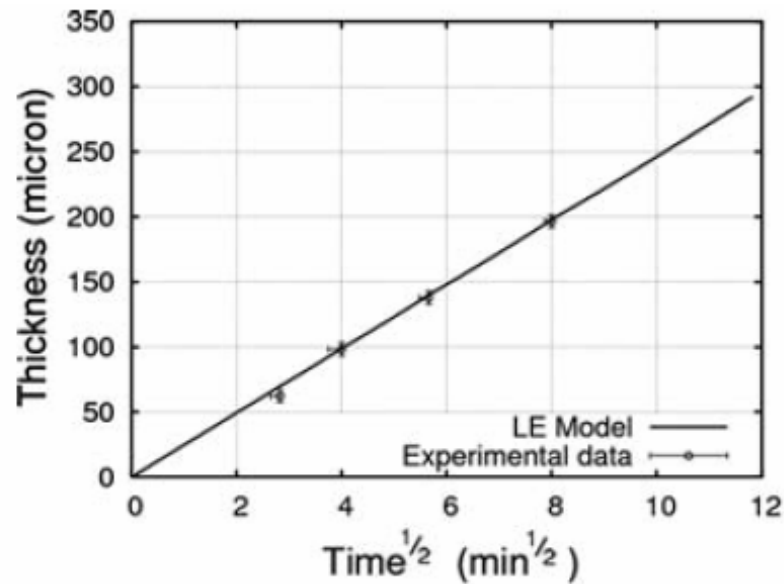


From: C. R. Hutchinson, H. S. Zurob, Y. Bréchet: Metall. Mater. Trans. (37A) 2006, 1711-1720.



Model 1: Sharp interface, infinite mobility LE(NP)

$\gamma \rightarrow \alpha$ transformation: Fe-C



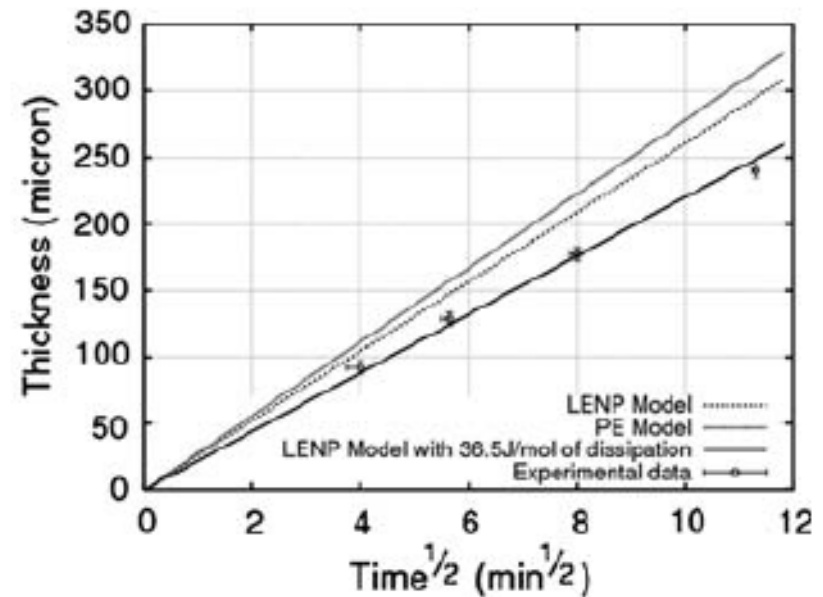
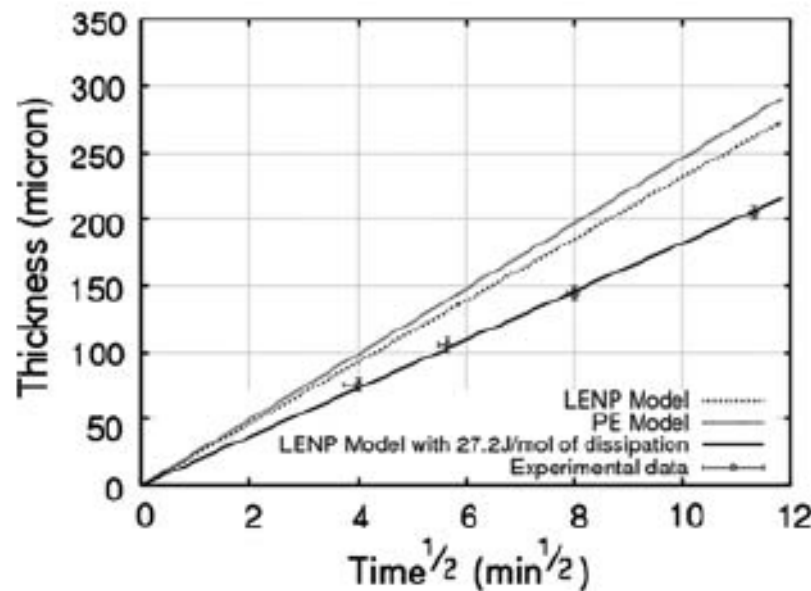
Ferrite layer growth kinetics during decarburization of an Fe-0.57C (mass frac. in %) binary alloy at 850°C and 825°C.

From: A. Béché, H. S. Zurob, C. R. Hutchinson: Metall. Mater. Trans. (38A) 2007, 2950-2955.



Model 1: Sharp interface, infinite mobility LE(NP)

$\gamma \rightarrow \alpha$ transformation: Fe-C-Cr

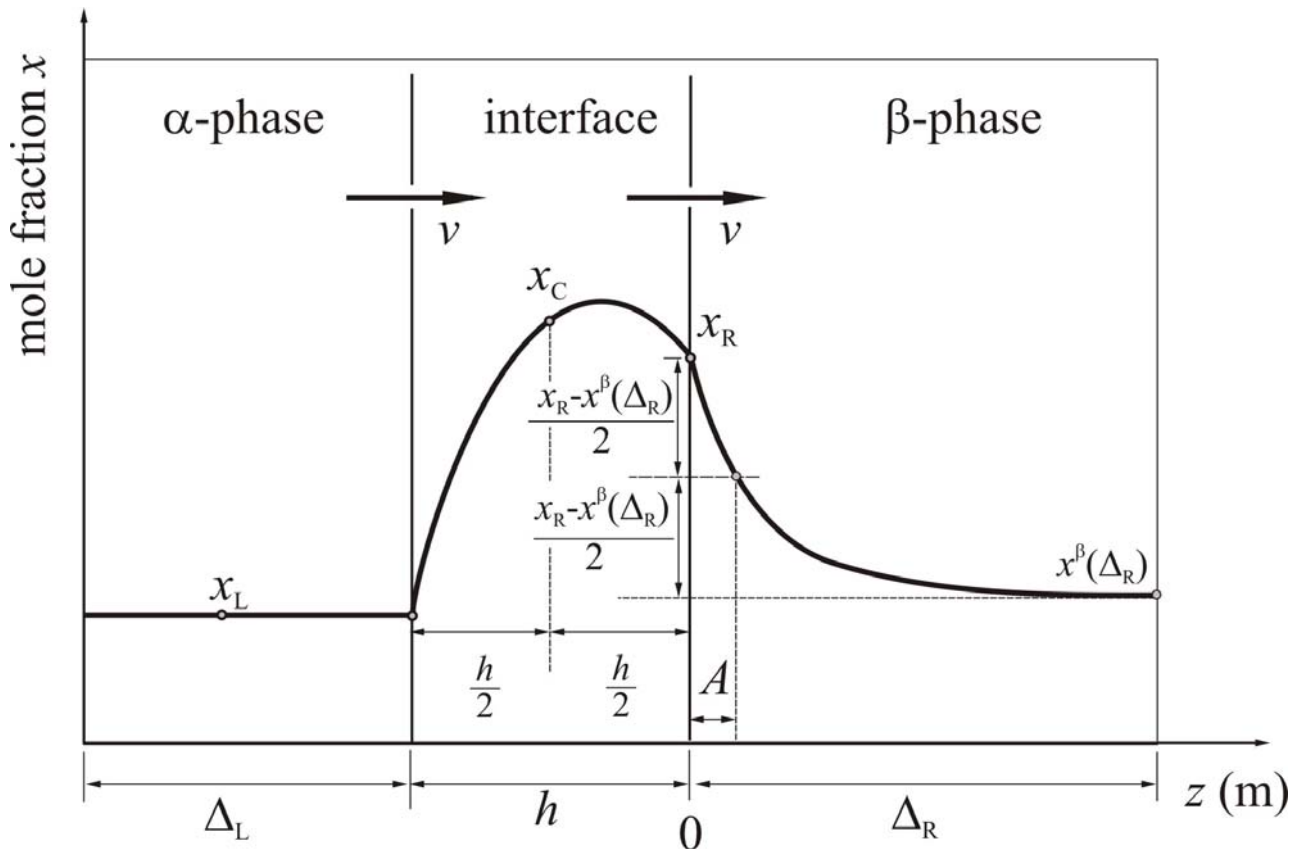


Ferrite layer growth kinetics during decarburization of an Fe-0.58C-2.0Cr (mass frac. in %) alloy at 806°C and 775°C.

From: A. Béché, H. S. Zurob, C. R. Hutchinson: Metall. Mater. Trans. (38A) 2007, 2950-2955.



Model 2: Thick interface parametric model

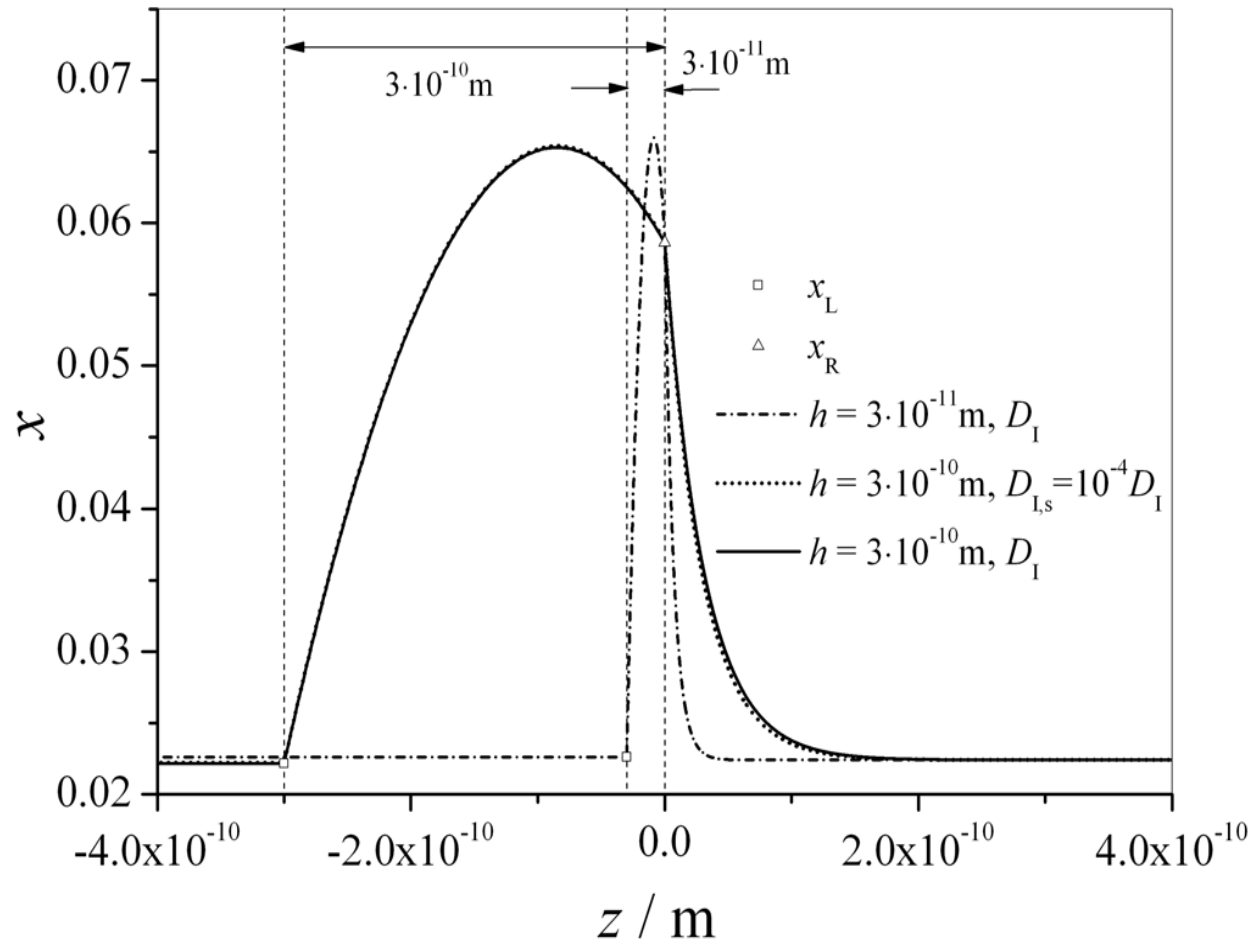


$$x^{\text{int}}(z) = 2 \left(x_L - 2x_C + x_R \right) \left(\frac{z}{h} \right)^2 + \left(x_L - 4x_C + 3x_R \right) \left(\frac{z}{h} \right) + x_R$$

$$x^\beta(z) = B \left(\exp\left(-\frac{z}{A}\right) + \exp\left(-\frac{2\Delta_R - z}{A}\right) \right) + x_{\text{start}}^\beta$$

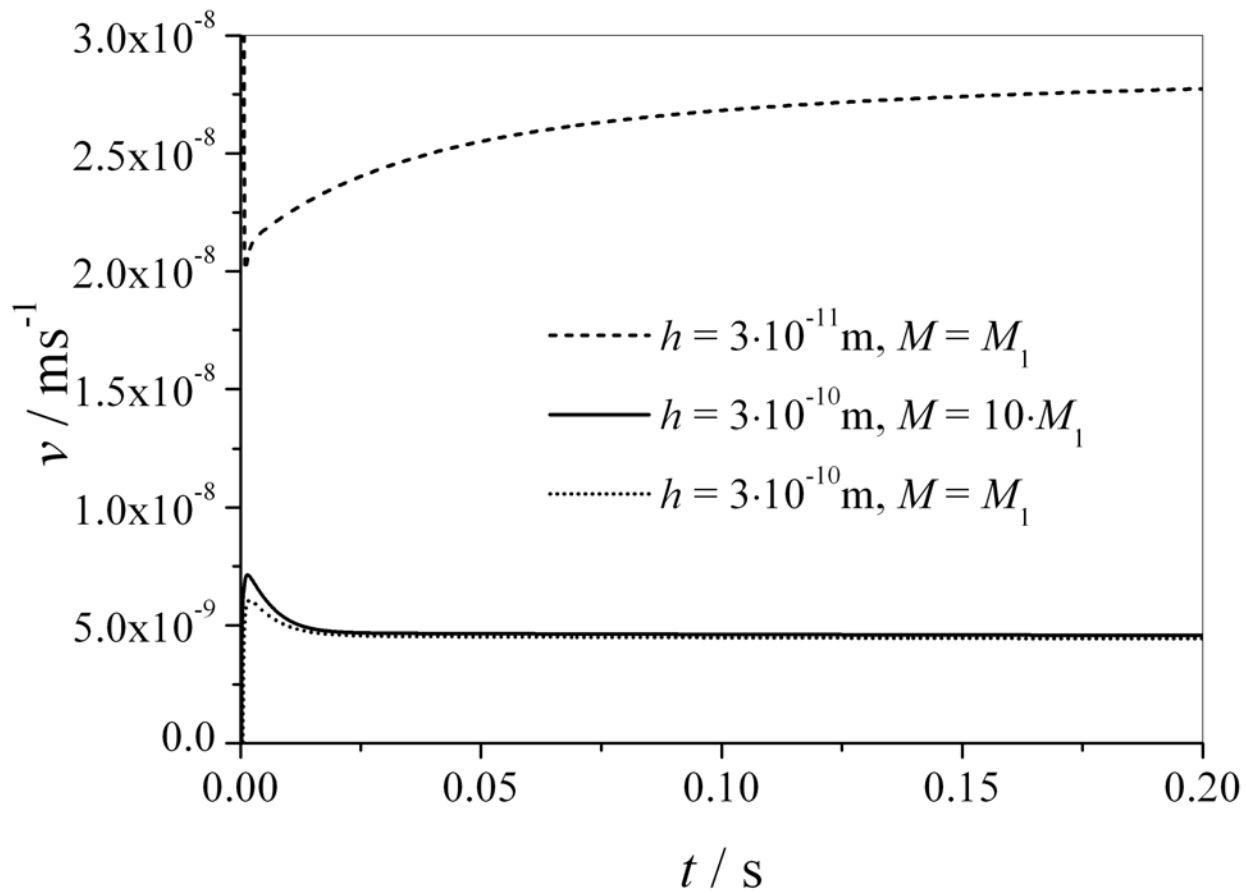


Model 2: Fe-Mn system



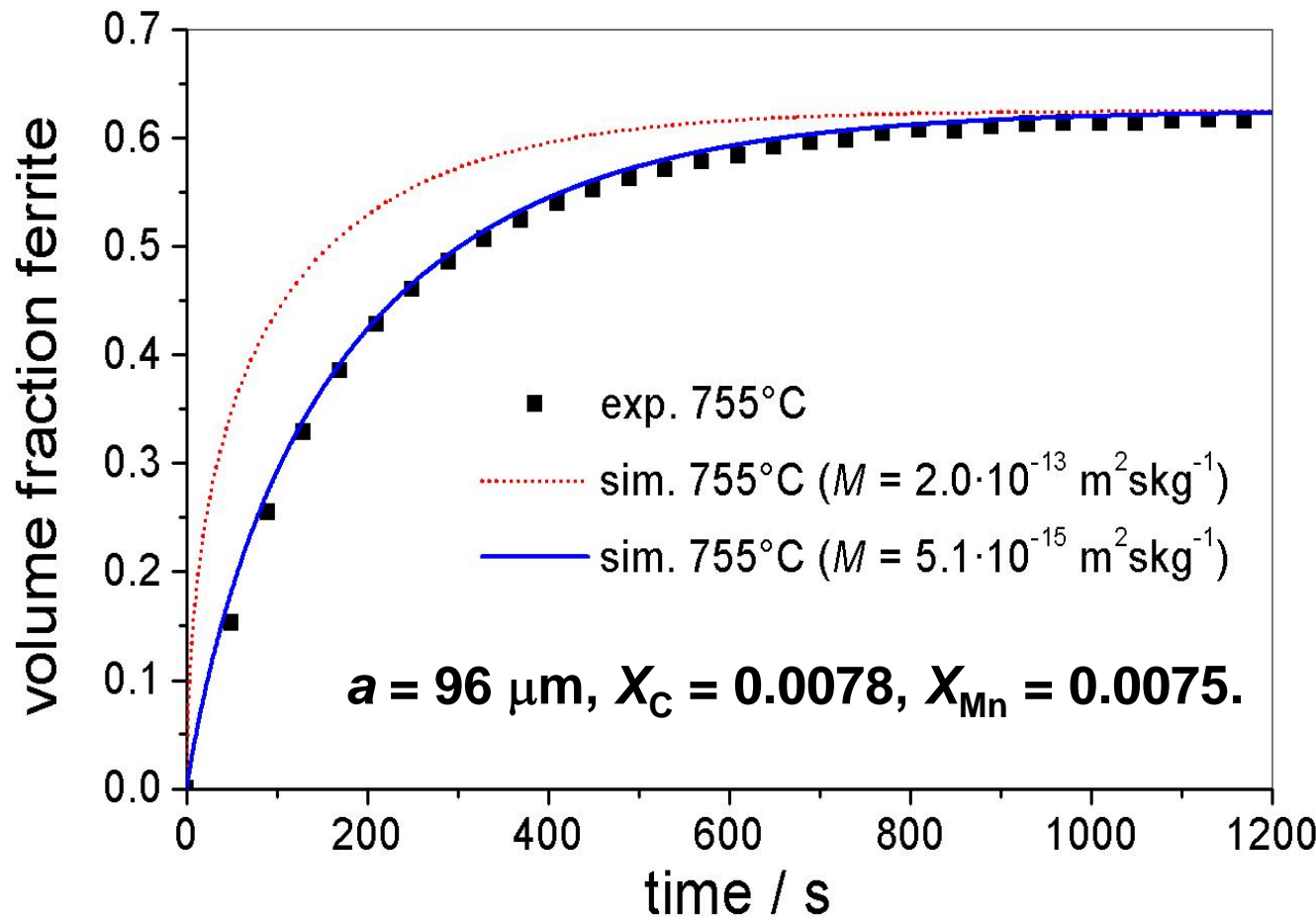


Model 2: Fe-Mn system



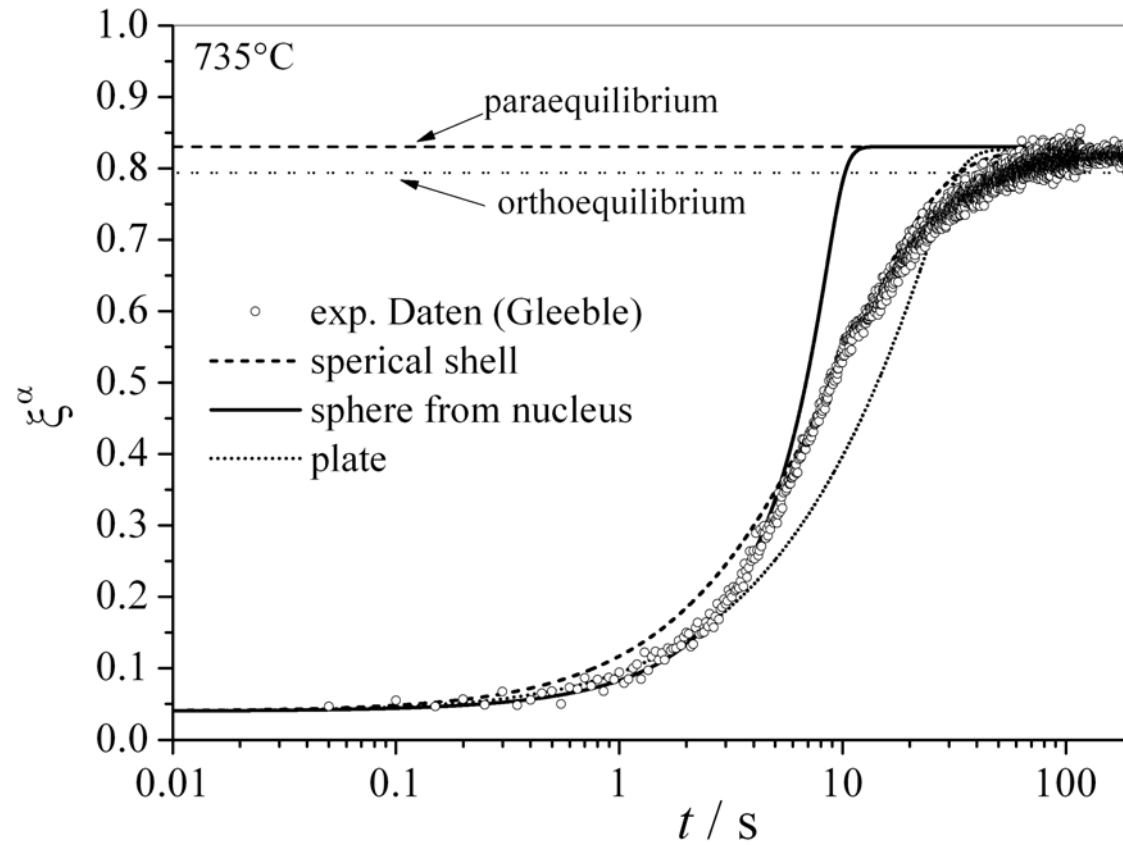


Model 3: Fe-Mn-C system





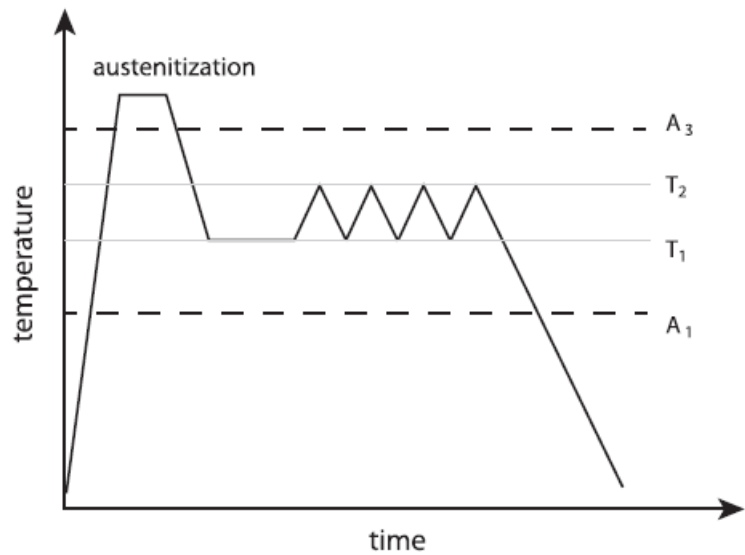
Model 3: (Fe-C-Mn-Si)



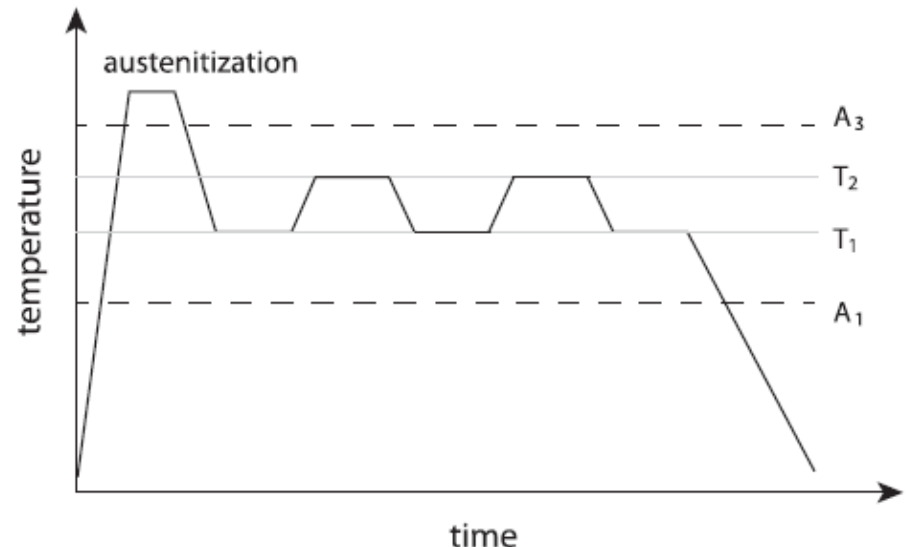


Novel experimental approach: Cyclic phase transformations

I-type experiment



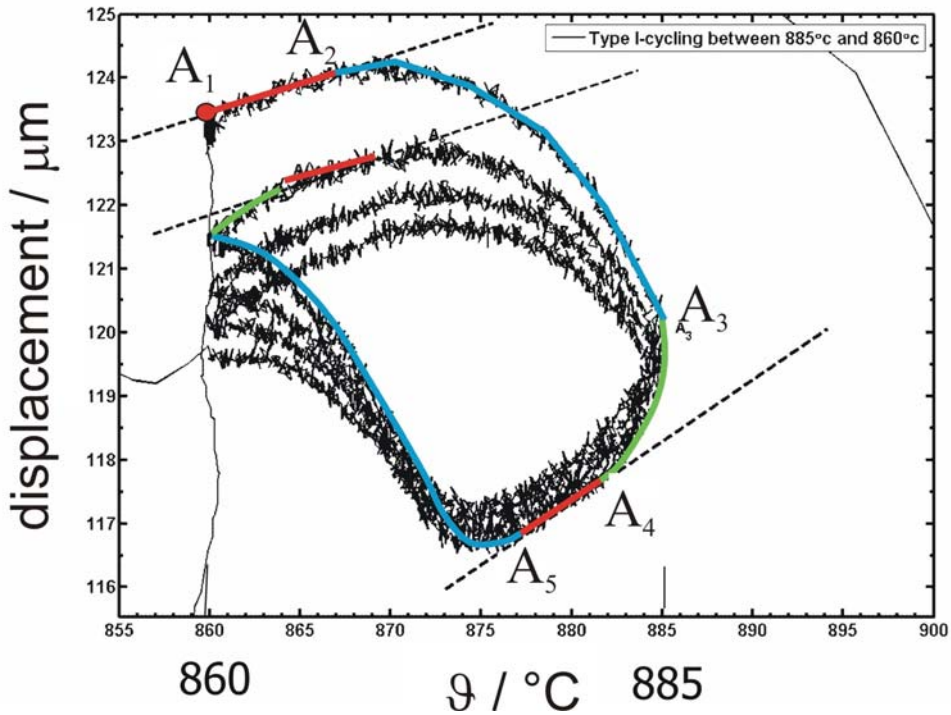
H-type experiment





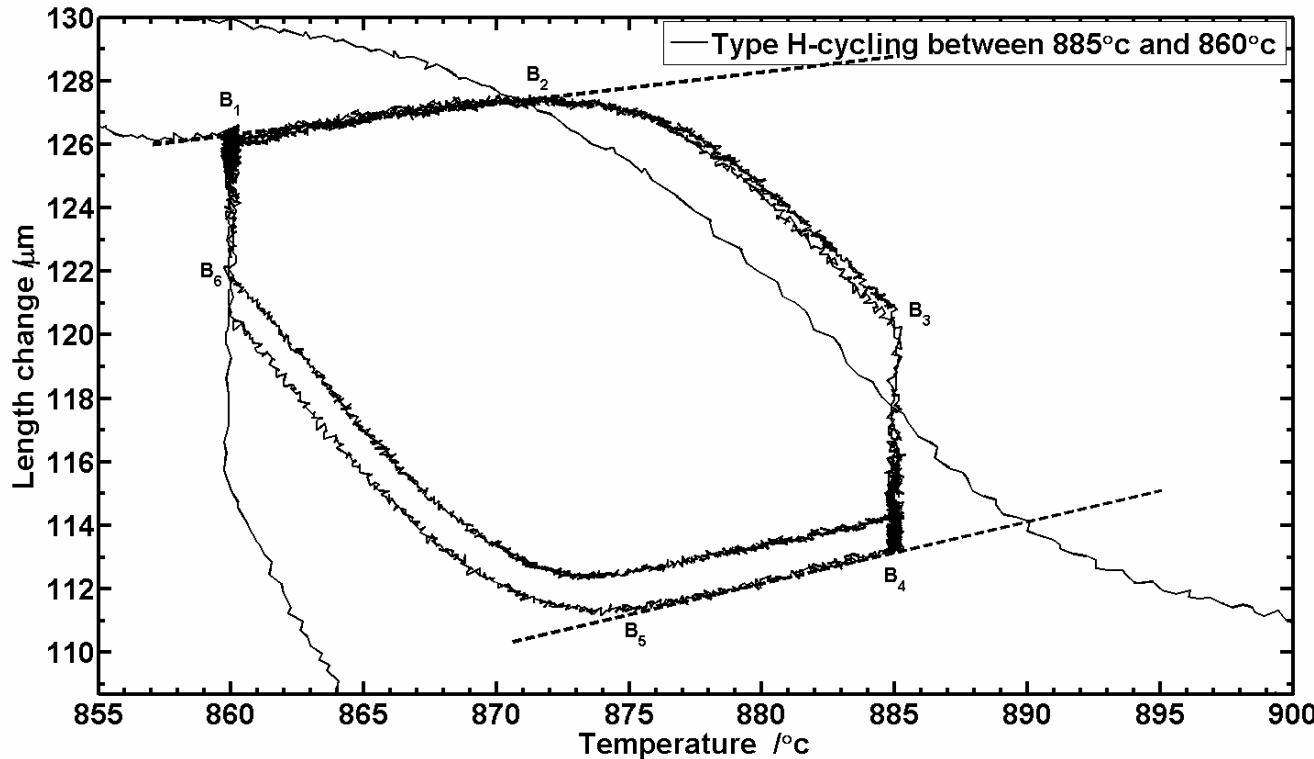
Novel experimental approach: Cyclic phase transformations

I-type experiment



A₁-A₂ and A₄-A₅: **stagnant stage**
A₃-A₄: **Inverse phase transformation**

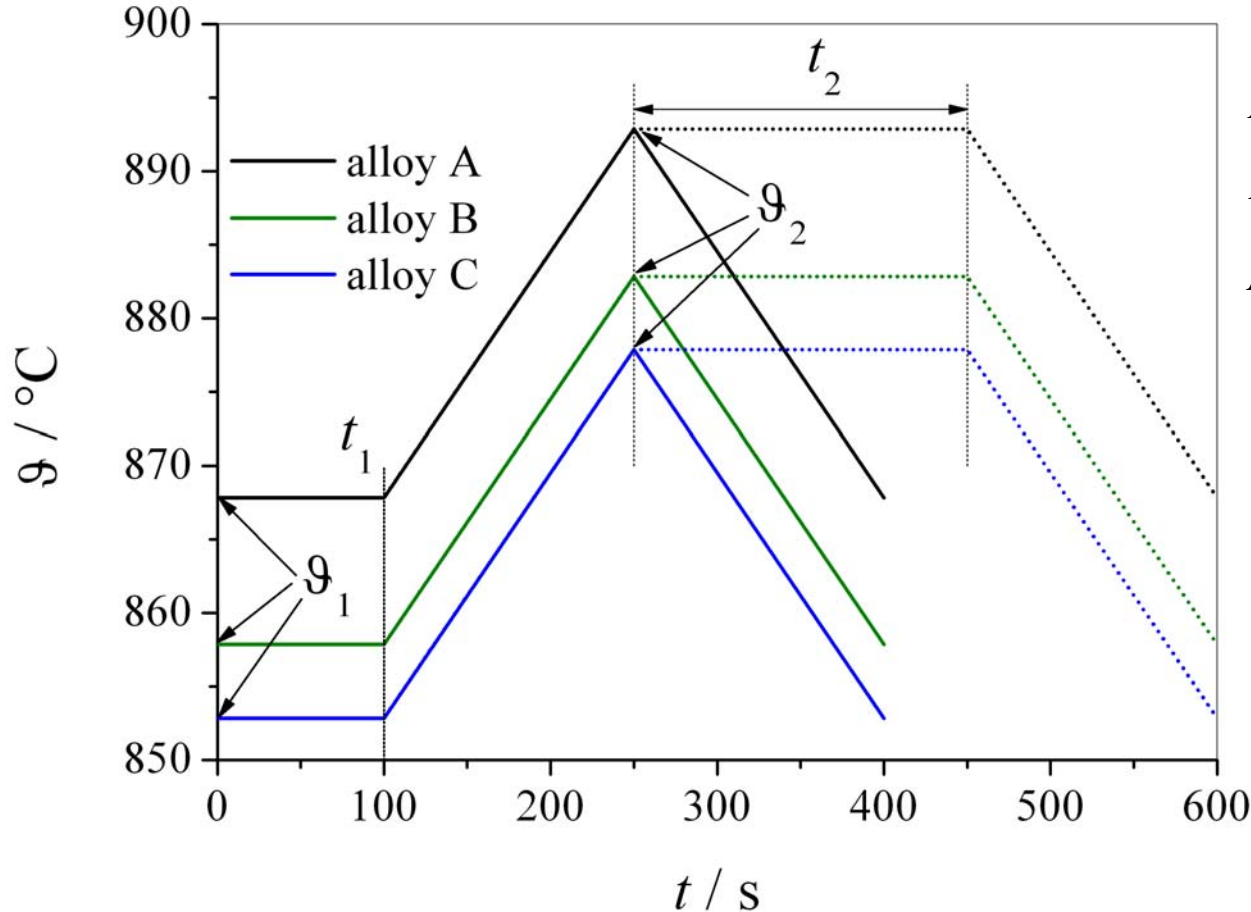
Novel experimental approach: Cyclic phase transformations



B₁-B₂ and B₄-B₅: stagnant stage



Heat treatment in the computer simulations



Alloy A: $w_{\text{Mn}} = 1 \cdot 10^{-3}$; $w_{\text{C}} = 2 \cdot 10^{-4}$

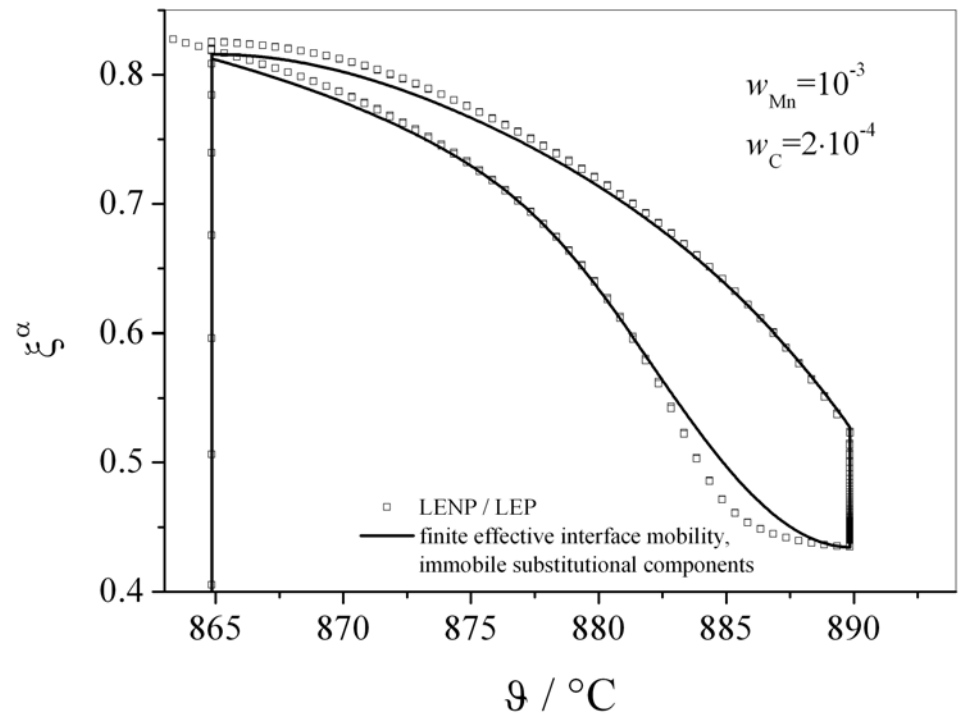
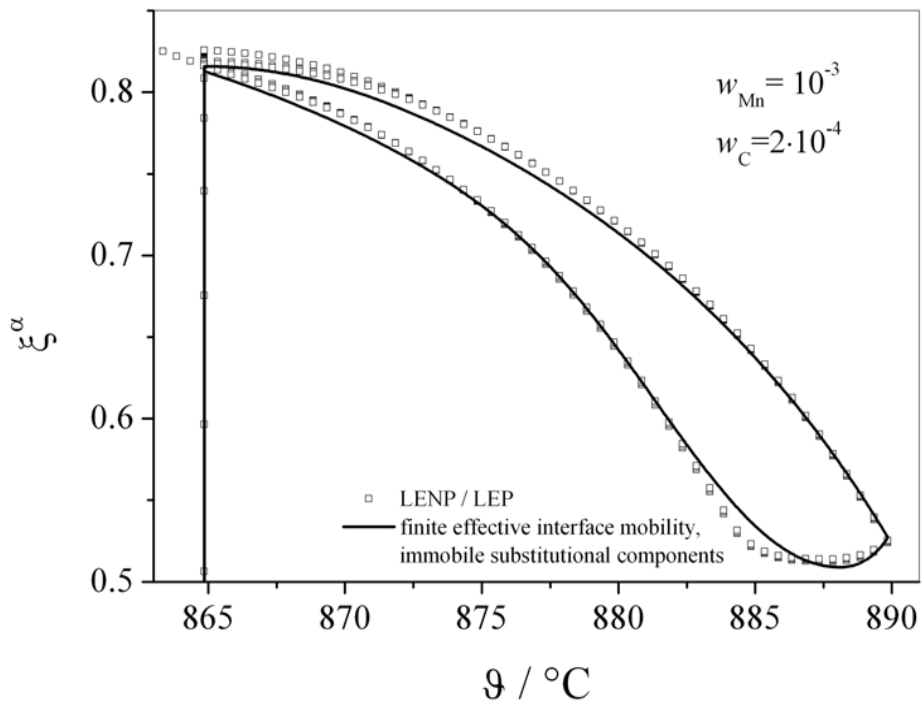
Alloy B: $w_{\text{Mn}} = 2 \cdot 10^{-3}$; $w_{\text{C}} = 2 \cdot 10^{-4}$

Alloy C: $w_{\text{Mn}} = 3 \cdot 10^{-3}$; $w_{\text{C}} = 2 \cdot 10^{-4}$



Comparison of Model 1 and Model 3

Alloy A:

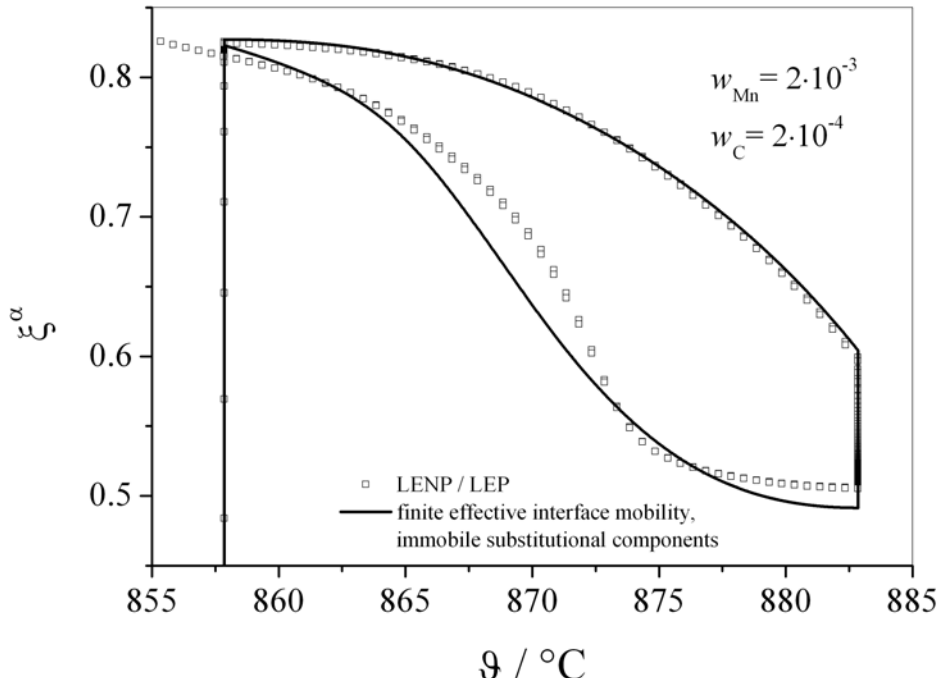
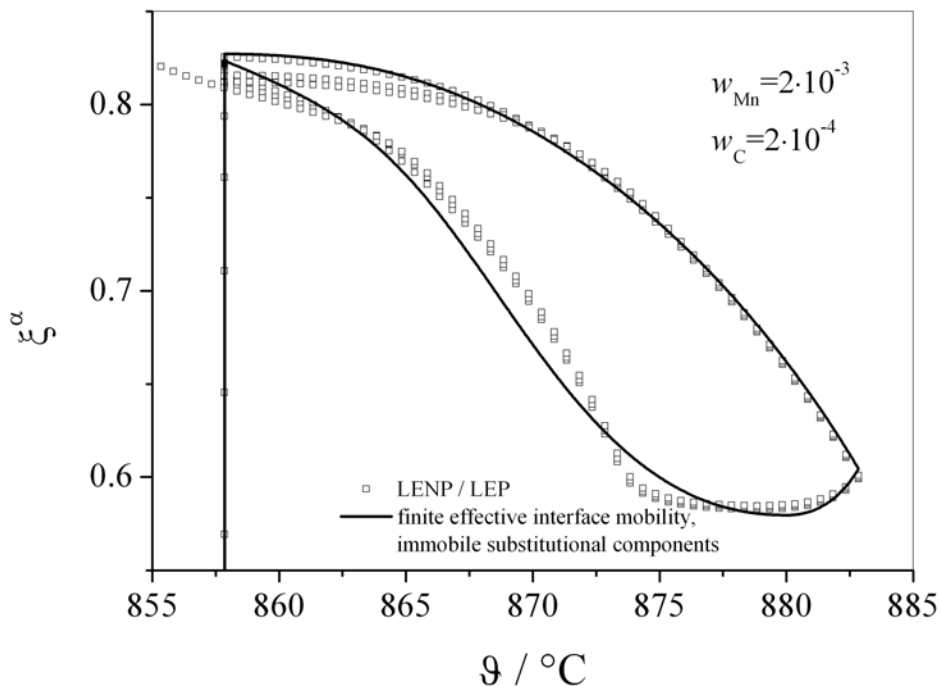


□ local equilibrium; — effective mobility



Comparison of Model 1 and Model 3

Alloy B:

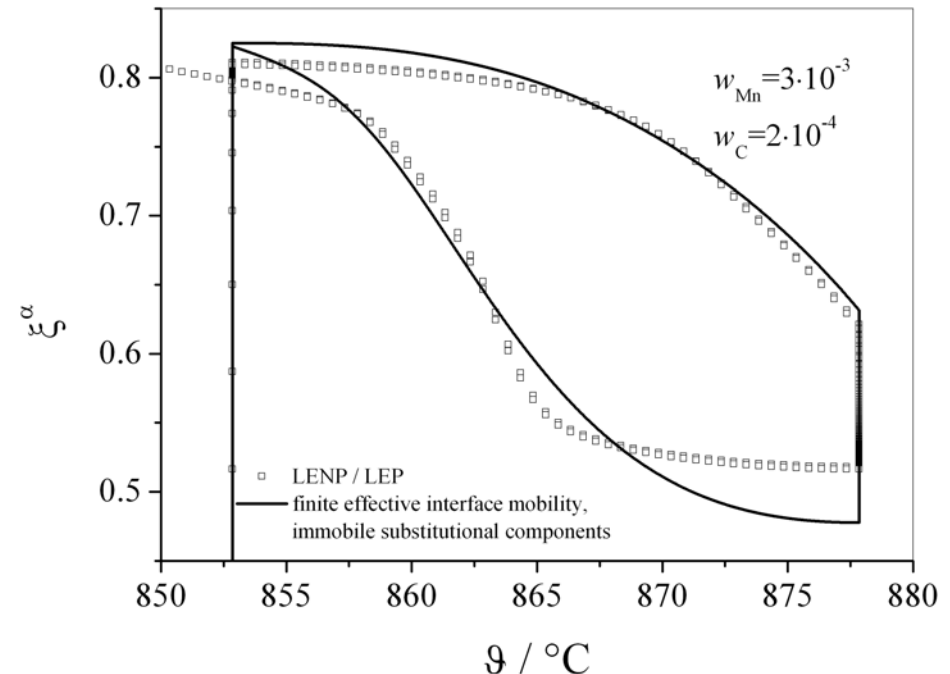
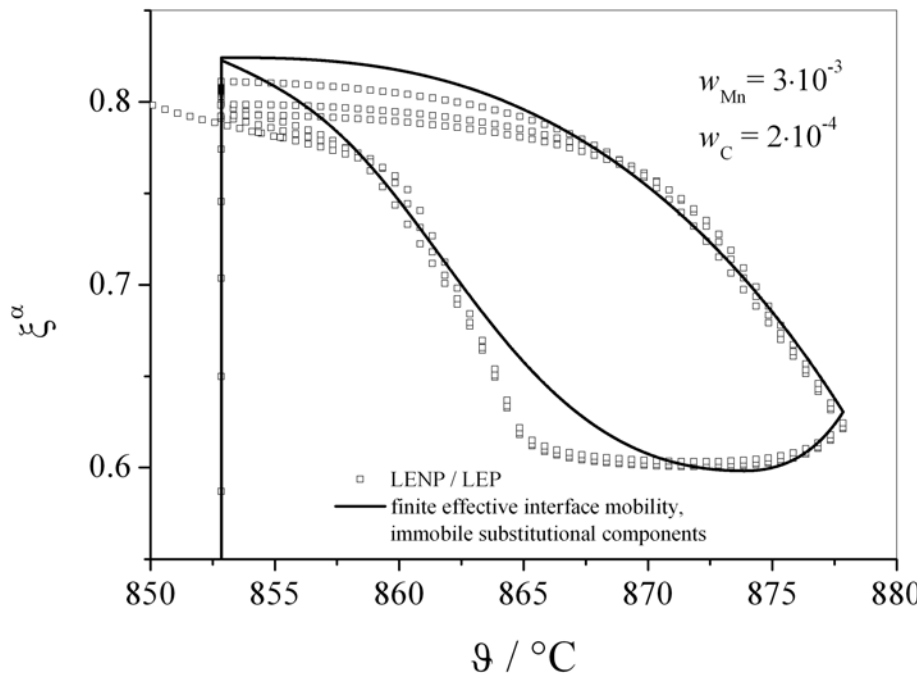


□ local equilibrium; — effective mobility



Comparison of Model 1 and Model 3

Alloy C:

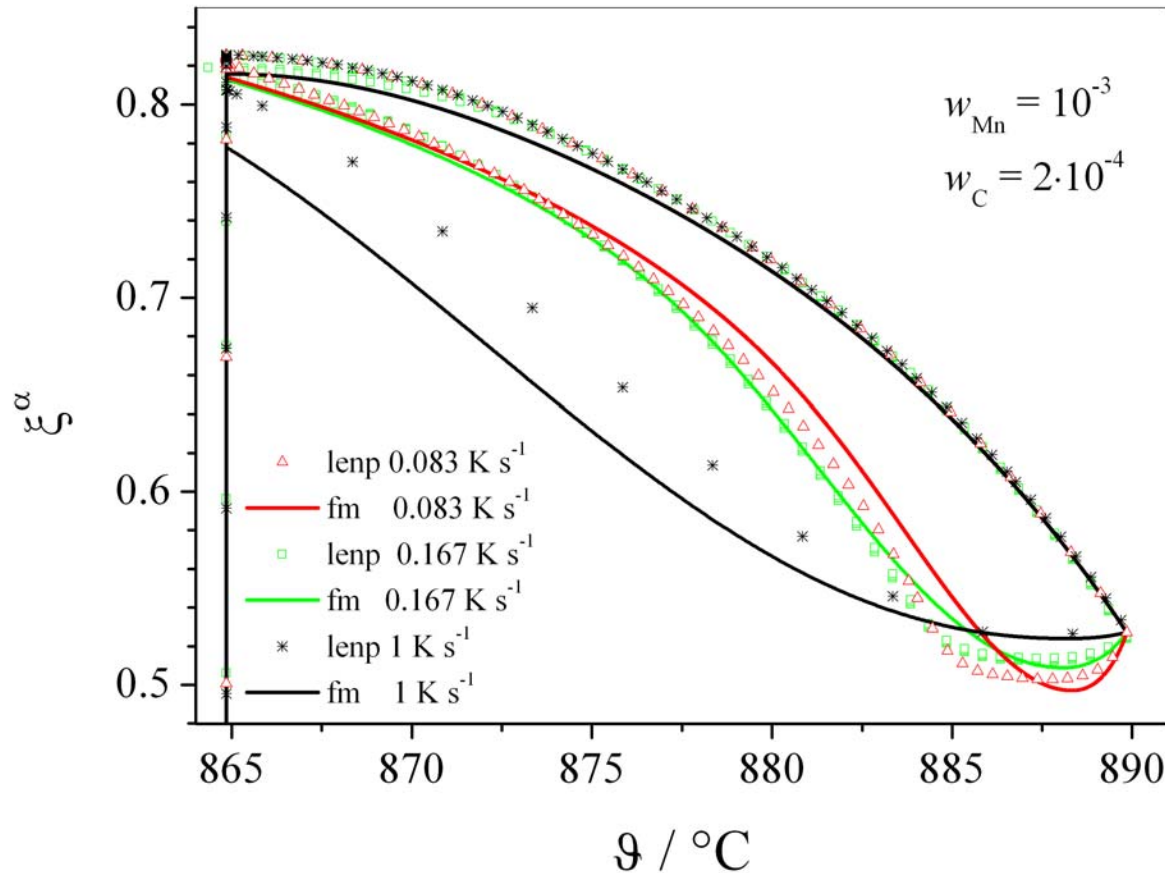


□ local equilibrium; — effective mobility



Comparison of Model 1 and Model 3

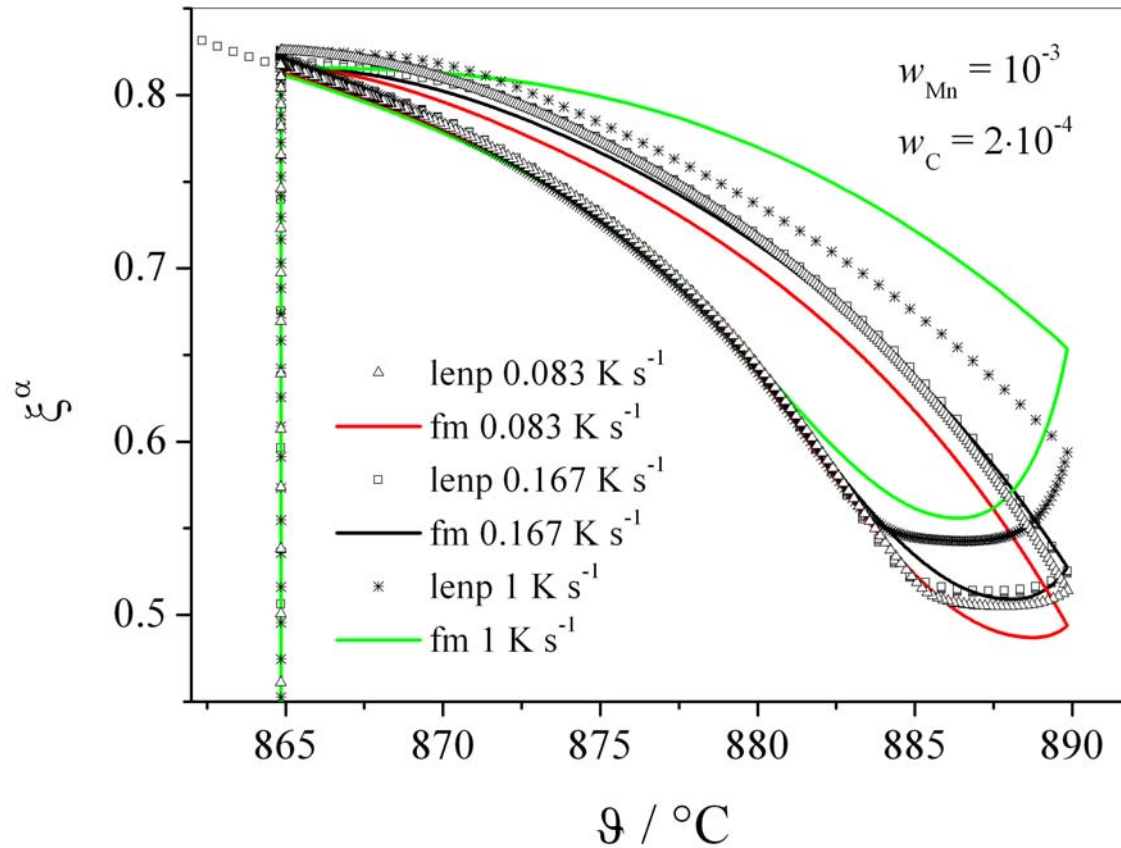
Different cooling rates:





Comparison of Model 1 and Model 3

Different heating rates:





Effective mobility

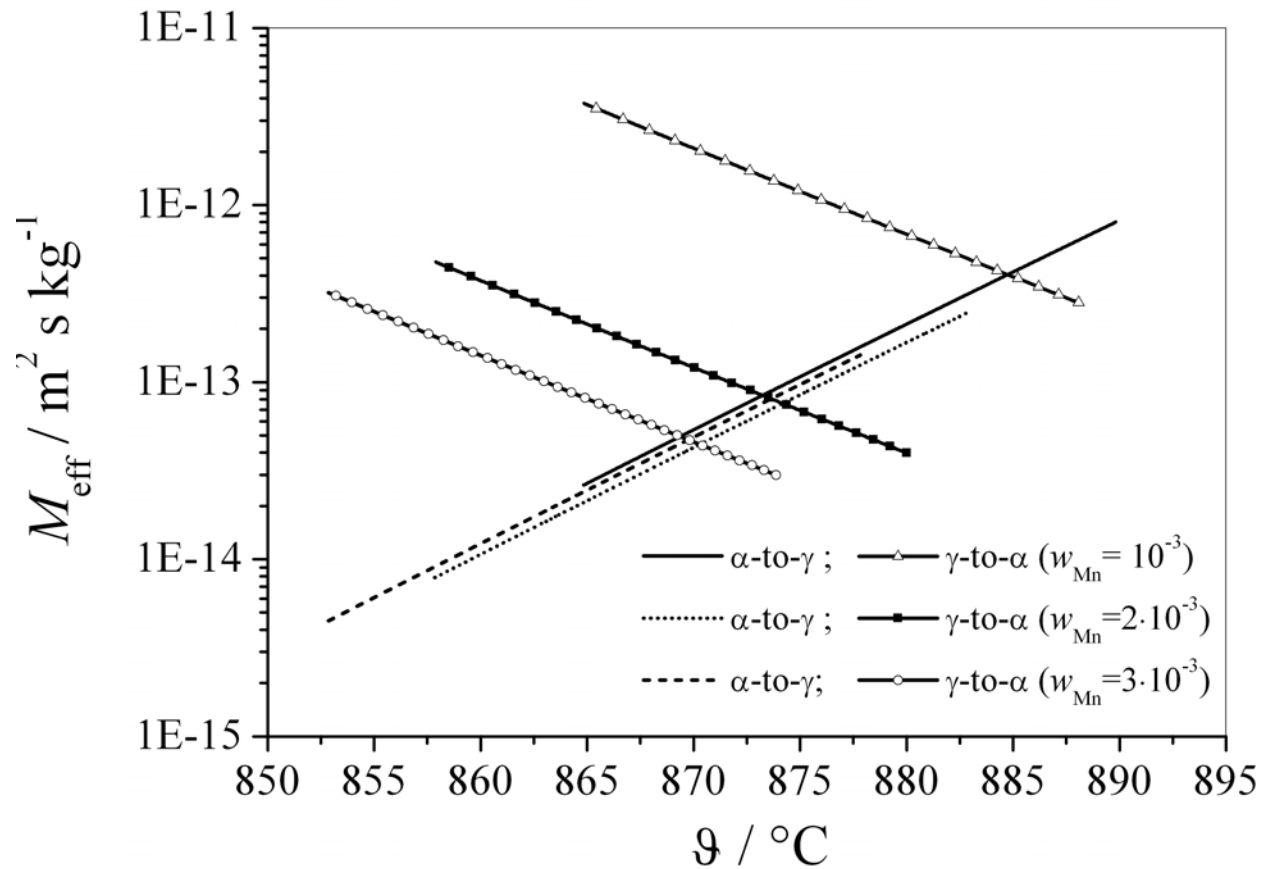
$$M_{\text{eff}} = M_0 \cdot \exp \left[\frac{1}{RT} (-Q + a(T - T_s)) \right] \quad Q = 140 \cdot 10^3 \text{ J mol}^{-1} \text{ K}^{-1}$$

Table 1: Coefficients for the different model alloys

	ϑ - range	T_s / K	M_0 / $\text{m}^2 \text{ s kg}^{-1}$	a / $\text{J mol}^{-1} \text{ K}^{-1}$	Composition
$\alpha \rightarrow \gamma$	$864.85^\circ\text{C} \leq \vartheta \leq 889.85^\circ\text{C}$	1138	$7 \cdot 10^{-8}$	$1.2 \cdot 10^3$	$w_{\text{Mn}} = 10^{-3}; w_{\text{C}} = 2 \cdot 10^{-4}$
$\gamma \rightarrow \alpha$	$864.85^\circ\text{C} \leq \vartheta \leq 889.85^\circ\text{C}$	1138	$1 \cdot 10^{-5}$	$-1.2 \cdot 10^3$	$w_{\text{Mn}} = 10^{-3}; w_{\text{C}} = 2 \cdot 10^{-4}$
$\alpha \rightarrow \gamma$	$857.85^\circ\text{C} \leq \vartheta \leq 882.85^\circ\text{C}$	1131	$2.3 \cdot 10^{-8}$	$1.2 \cdot 10^3$	$w_{\text{Mn}} = 2 \cdot 10^{-3}; w_{\text{C}} = 2 \cdot 10^{-4}$
$\gamma \rightarrow \alpha$	$857.85^\circ\text{C} \leq \vartheta \leq 882.85^\circ\text{C}$	1131	$1.4 \cdot 10^{-6}$	$-1.2 \cdot 10^3$	$w_{\text{Mn}} = 2 \cdot 10^{-3}; w_{\text{C}} = 2 \cdot 10^{-4}$
$\alpha \rightarrow \gamma$	$852.85^\circ\text{C} \leq \vartheta \leq 877.85^\circ\text{C}$	1126	$1.4 \cdot 10^{-8}$	$1.2 \cdot 10^3$	$w_{\text{Mn}} = 3 \cdot 10^{-3}; w_{\text{C}} = 2 \cdot 10^{-4}$
$\gamma \rightarrow \alpha$	$852.85^\circ\text{C} \leq \vartheta \leq 877.85^\circ\text{C}$	1126	$1 \cdot 10^{-6}$	$-1.2 \cdot 10^3$	$w_{\text{Mn}} = 3 \cdot 10^{-3}; w_{\text{C}} = 2 \cdot 10^{-4}$



Effective mobility





Comparison with experimental data

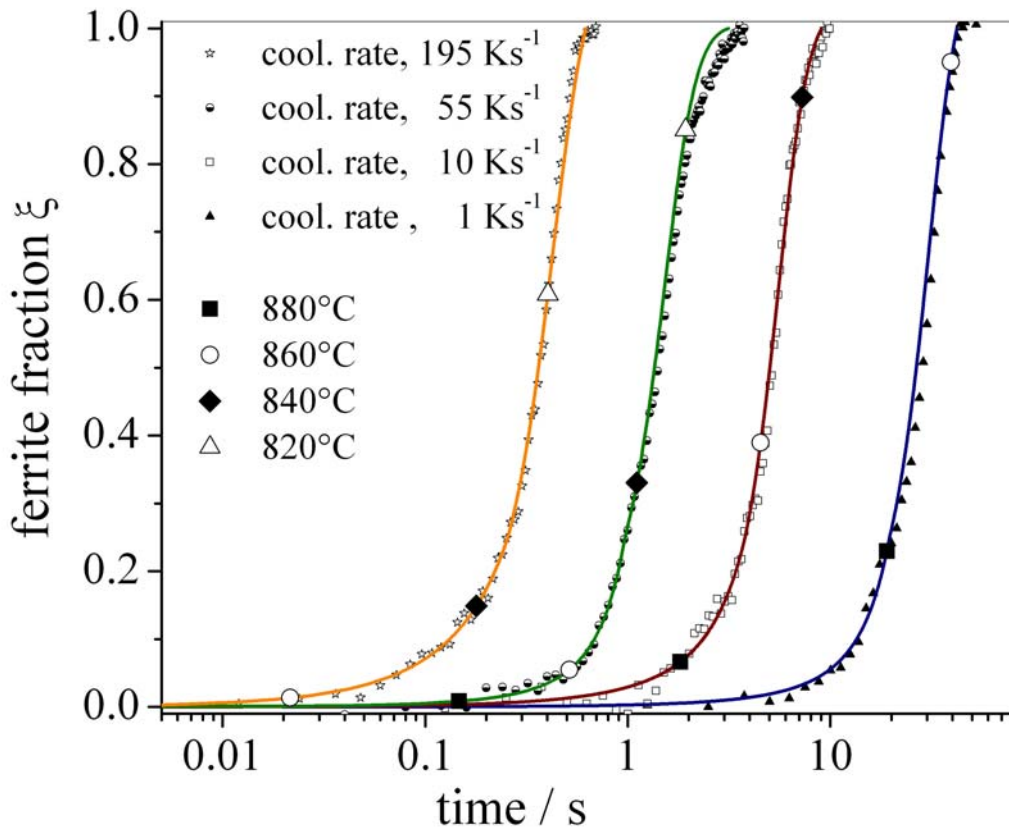


Table 1
Chemical composition of the investigated steel

C	Mn	P	S	Si	Ti	Nb	Al	N
0.002	0.11	0.01	0.008	0.01	0.059	0.009	0.033	0.0041

Values are mass fractions in %.

$$\xi(t) = \frac{a}{1 + b \exp(-ct)}$$

$$\frac{d\xi}{ds} \cdot \frac{ds}{dt} = \frac{d\xi}{ds} (\text{geometry}) \cdot \frac{ds}{dt}$$

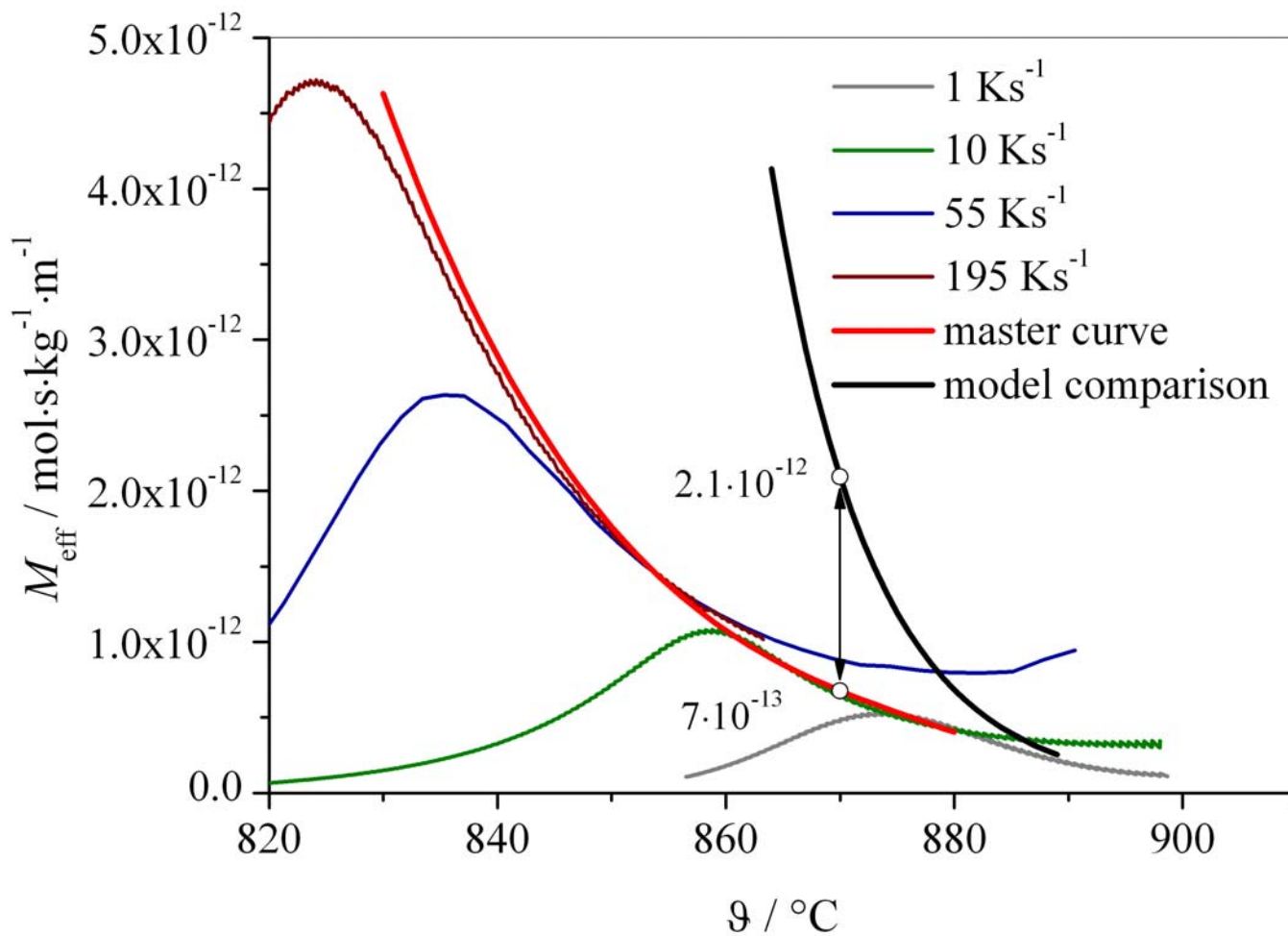
$v = M_{\text{eff}} \cdot \Delta G$

M. Militzer, Austenite decomposition kinetics in advanced low carbon steels, Solid Phase Transformations 99, eds. M. Koiwa, K. Otsuka and T. Miyazaki, JIM, Sendai (1999) 1521-1524.

E. Gamsjäger, M. Militzer, F. Fazeli, J. Svoboda, F. D. Fischer: "Interface mobility in case of the austenite-to-ferrite phase transformation", *Comp. Mat. Sci.*, (2006) 94 -100.

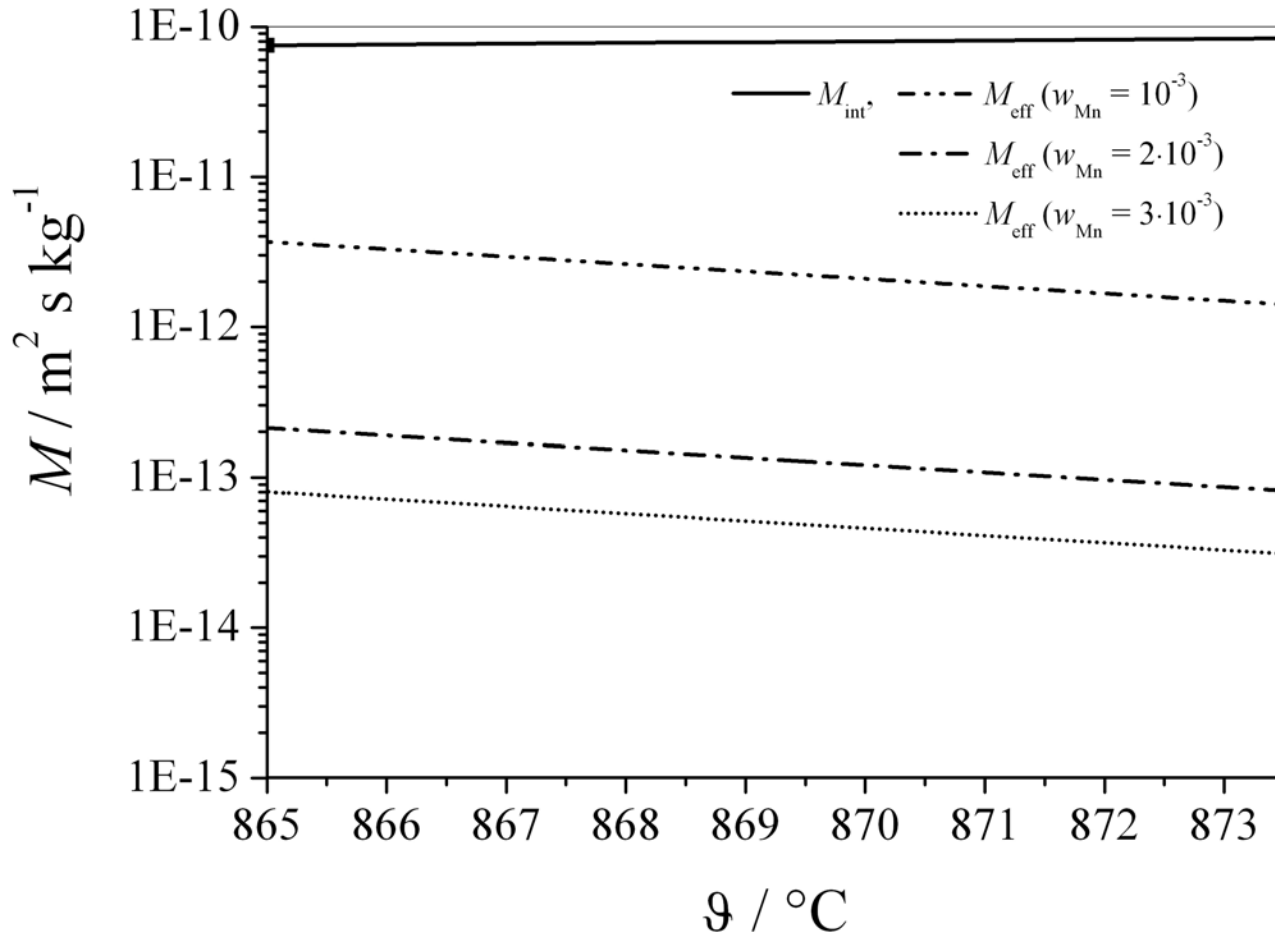


Comparison with experimental data



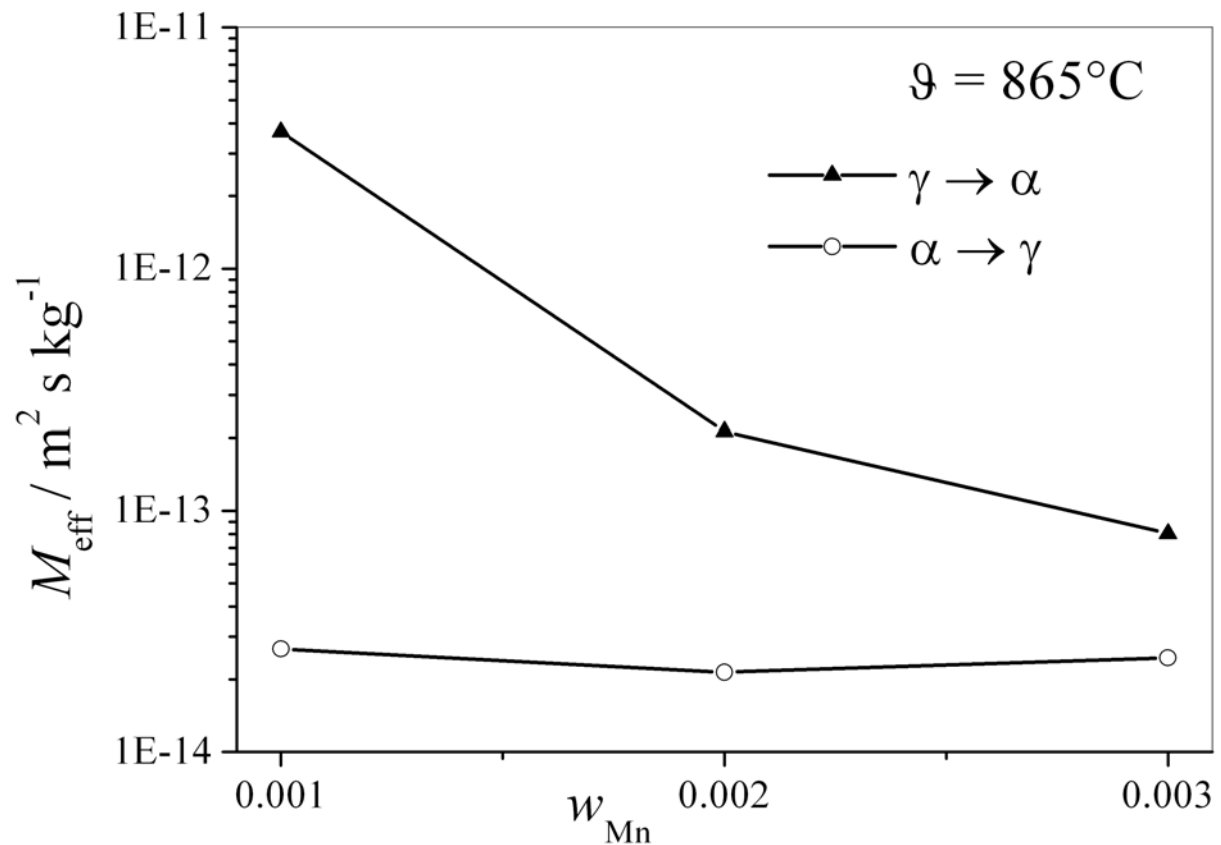


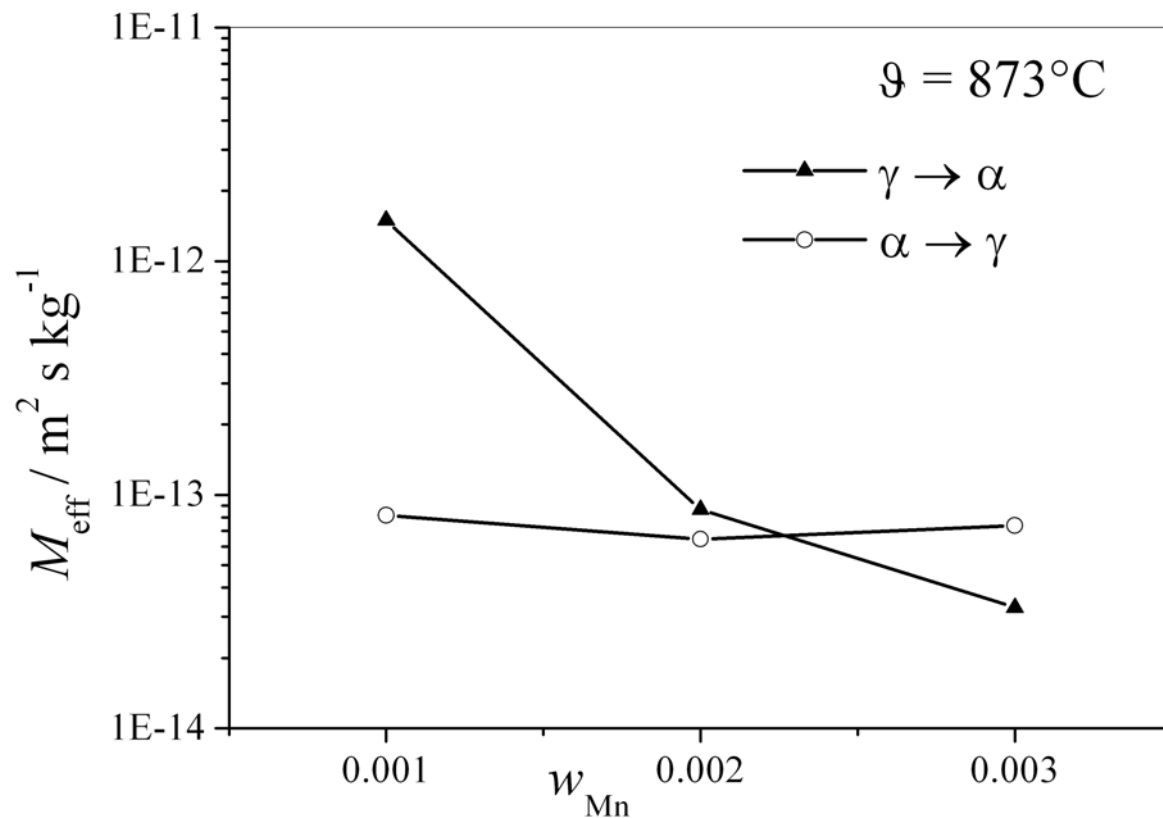
Comparison with intrinsic mobility



[1] M. Hillert, L. Höglund, *Scrip. Mater.* (2006), 54, 1259-1263.

[2] E. Gamsjäger, *Habilitation treatise* (2008), Montanuniversität Leoben







Conclusions and Outlook

- **Thick interface parametric model**
 - *Substitutional diffusion in the interface*
 - *C-diffusion in bulk*

} are rate-controlling.
 - **Simplified model**
 - *Comparison with experimental results.*
 - **Prediction of the γ / α transformation kinetics**
 - *Effective mobility as a function of composition and temperature by comparison with LE-model and experiments.*
-

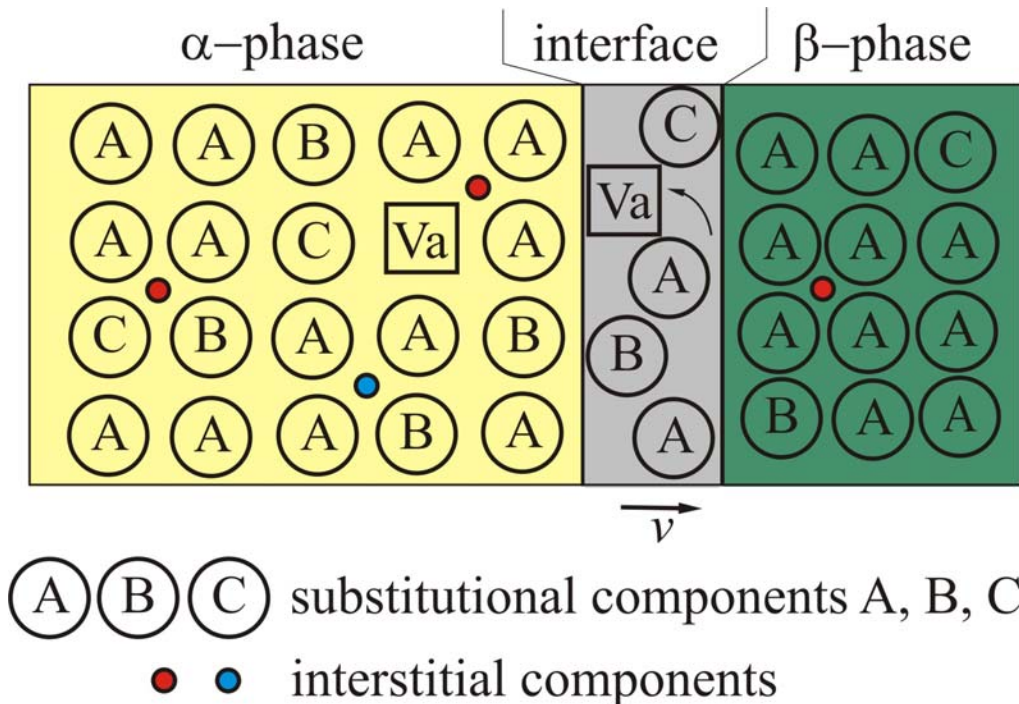


Kinetics of diffusive phase transformations

Transformation kinetics depends on:

- 1, Diffusion processes of the components in the bulk materials,
- 2, the rearrangement of the lattice and
- 3, on diffusion processes in the interface.

2+3: interfacial reaction





Gibbs energy G and dissipation Q

$$G = \frac{1}{\Omega} \int_{-\Delta_L - h}^{\Delta_R} (x\mu_1 + (1-x)\mu_2) dz = \underbrace{\frac{1}{\Omega} \int_{-\Delta_L - h}^0 (x\mu_1 + (1-x)\mu_2) dz}_{G^{\alpha+I}} + \underbrace{\frac{1}{\Omega} \int_0^{\Delta_R} (x\mu_1 + (1-x)\mu_2) dz}_{G^\beta}$$

$$Q = RT\Omega \int_{-(\Delta_L + h)}^{\Delta_R} \left(\frac{1}{xD_1} + \frac{1}{(1-x)D_2} \right) j^2 dz$$

↓

$$G = G(x_L, x_R, A, \Delta_R)$$

$$Q = Q(\dot{x}_L, \dot{x}_R, \dot{A}, v)$$

$$\frac{1}{2} \frac{\partial Q}{\partial \dot{x}_L} = - \frac{\partial G}{\partial x_L}$$

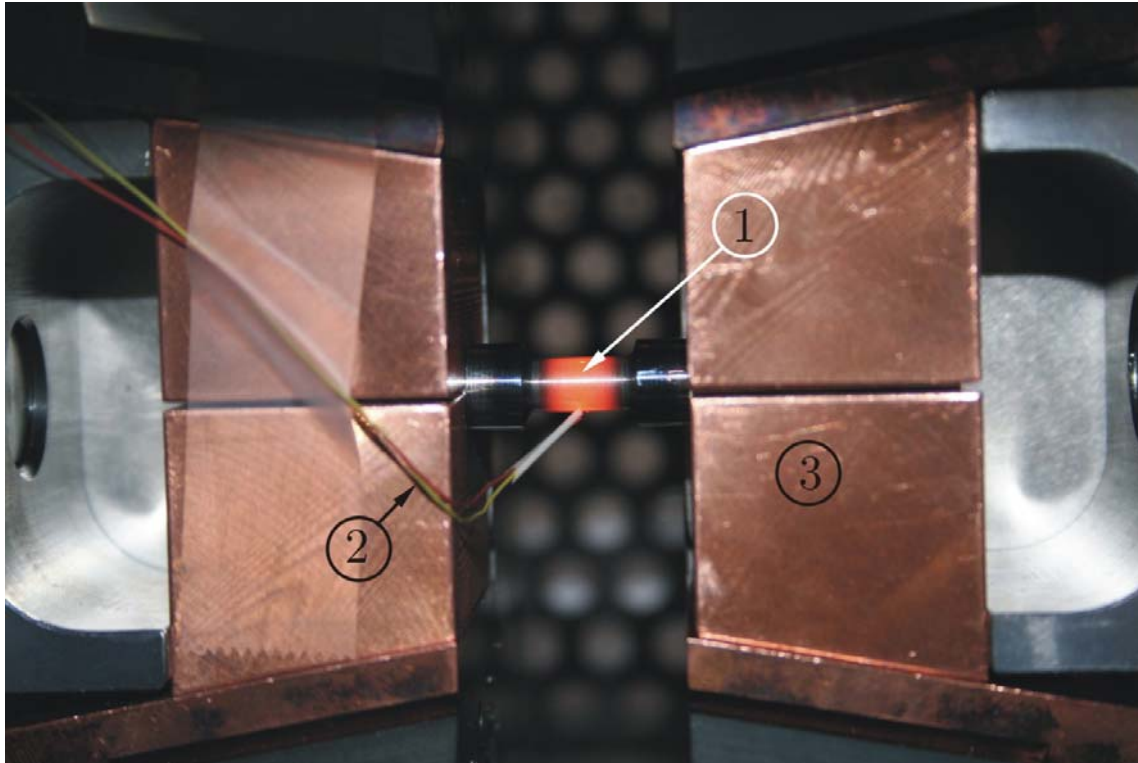
$$\frac{1}{2} \frac{\partial Q}{\partial \dot{x}_R} = - \frac{\partial G}{\partial x_R}$$

$$\frac{1}{2} \frac{\partial Q}{\partial v} = \frac{\partial G}{\partial \Delta_R}$$

$$\frac{1}{2} \frac{\partial Q}{\partial \dot{A}} = - \frac{\partial G}{\partial A}$$



Experimental setup



- 1... Heated specimen
- 2 ... Electric supply for the thermocouple
- 3 ... Cu jaws



Composition, heat treatment and microstructure

Table: Composition of the 10MnSi7 steel grade

	C	Mn	Si	P	S	Cr	Ni	Al	Ti	V	Nb
$x_i \cdot 100$	0.4173	1.6259	1.9802	0.0219	0.0124	0.0318	0.0188	0.0592	0.0460	0.0054	0.0018

